orbit is dependent on the strength and frequency of disturbances.

Propellant storage is a critical consideration. A gaseous propellant fills its storage volume uniformly if isothermal, and intolerable temperature gradients can be avoided. Liquids and solid propellants present a problem, but the changes and uncertainties may be acceptable if they are relatively constant and the satellite is spun. Two toroidal propellant tanks may be used to a) locate the mass center of the propellant at the proof mass to avoid propellant waste due to the gradient in the gravity field and to prevent coupling with the rotational dynamics of the satellite and b) minimize the gradient in the mass attraction field.

When the satellite's orientation is fixed relative to the local orbit coordinates, a mass attraction force or other body-fixed disturbance on the proof mass can produce a significant disturbance. If, on the other hand, a satellite is rotated, the average effect of these disturbances can be made smaller by an order of magnitude or more. Because of the cost required to reach a $10^{-11}g$ uncertainty level in the mass attraction of a proof mass, the rotation of a satellite about either the vertical or the normal to the orbit plane is highly desirable. This, of course, places requirements on the speed of response and the acceptable time delays of the control system, and in particular the thrustors.

Initial settling, control bandwidth and time delay

The dynamics of the motions of the satellite with respect to the proof mass is straightforward if both have the same gravity or are in a field-free space. This approximation is valid if the acquisition and settling takes place in a time which corresponds to a small change in central angle of the orbit; the orbital coupling of the horizontal and vertical motions can be neglected. If 200 sec is taken as a nominal settling time, the bandwidth of a linear system would be 3×10^{-2} rad/sec. In a nonlinear controller, some equivalent measure could be used.

If we arbitrarily require that the time delay τ reduces the phase margin less than 0.1 rad near the crossover frequency ω_x, then $\tau < 0.1/\omega_x$, and τ should be less than 3 sec for the settling behavior. Similarly, if we require $\tau < 0.1/\omega_s$ for spinning satellites, and ω_s could be as high as 1 rad/sec, we require $\tau < 0.1$ sec.

Disturbances

Thermal distortions in the satellite may change the effective null point of the pickoff by a discrete amount each time the satellite enters and leaves the sunlight. It is important to keep the impulse required to respond to this change small compared with the total impulse required to counteract the external disturbing forces. Regardless of the control mechanization involved, the impulse requirement is of the order of $\Delta V \approx 4d\omega_x$, where d is the amplitude of the sudden change in the null location. There are variations of a factor of 2 or 3 for different control mechanizations. Assuming a settling time of 100 sec, the allowable thermal distortion of the satellite to maintain $\Delta V < 4 \times 10^{-5}$ m/sec would be a displacement of 1 mm.

The total impulse required to counteract an external impulse or step change in the external force should be independent of bandwidth as long as the mechanization is adequately damped.

References

[1] Lange, B. O., "The Drag-Free Satellite," *AIAA Journal*, Vol. 2, No. 9, Sept. 1964, pp. 1590–1606.

[2] Moe, O. K., "A Review of Atmospheric Models in the Altitude Range 100 to 1000 km.," AIAA Paper 69-50, New York, 1969.

[3] DeBra, D. B., "A Comparison of Satellite Drag Measurement Techniques," paper presented at the IInd International Conference on Space Engineering, Venice, Italy, May, 1969.

[4] "Final Report on a Study to Prepare a Preliminary Analysis and Design Definition of a Drag-Free Satellite for Geodynamics," submitted to NASA under Contract NSR-05-020-379 by Stanford Univ., Aug. 1970, Guidance & Control Lab., Stanford, Calif.

[5] Fleming, A. W., "Mass Attraction Properties of Drag-Free Satellites," Dept. of Aeronautics and Astronautics, Stanford Univ., Stanford, Calif., to be published.

Life Test Summary and High-Vacuum Tests of 10-mlb Resistojets

RONALD Y. YOSHIDA,* CARL R. HALBACH,† AND C. SCOTT HILL‡

The Marquardt Company, Van Nuys, Calif.

THIS Note summarily describes the results of an 8,000-hr life test of six 10-mlb-thrust, high-temperature (2400°K) evacuated-concentric-tubes type resistojets and presents details of a high-vacuum test that was conducted on one of the resistojets to document the effect of cell pressure on thrust. Reference 1 describes the evacuated-concentric-tubes resistojet concept. This resistojet, in the ten-mlb-thrust size, is being developed primarily for use on manned space stations for drag make-up and for attitude control in conjunction with control-moment gyros. This Note describes resistojets with heater elements made of rhenium to be used with hydrogen and ammonia propellants. Reference 1 describes the development of related resistojets for use with bio-waste propellants.

Life Test Summary

The life test was comprised of the simultaneous testing of a cluster of six resistojets; four were operated with NH_3 and two with H_2. A 50/50 duty cycle-one cycle per hour, with the thrusters in two groups, two NH_3 and one H_2 thruster per group, was used. The four NH_3 thrusters were cycled in excess of 8000 hr. Anomalies occurred with the H_2 thrusters (S-1 and S-2) which are attributed to experimental fabrication techniques and not associated with the hydrogen propellant; thruster S-1 developed a leak and was left in the life test to obtain temperature data, and thruster S-2 was removed from the life test after 1426 hr. Another thruster, B-2, was substituted for S-2 and successfully completed 6023 hr of operation with hydrogen, at which time the life test was termi-

Table 1 Nominal values for life-test thrusters

Thruster serial no.	S-1	S-2	B-2	S-3	S-4	S-5	S-6
Propellant	H_2	H_2	H_2	NH_3	NH_3	NH_3	NH_3
Test duration, hr	7858	1426	6023	8048	8152	8052	8134
I_{sp}, sec (estimated for space)	660	670	670	320	320	320	320
Electric power, w	258	220	222	131	189	145	145
Thrust, mlb	11.7	10.0	10.5	9.2	11.9	10.6	10.5

Presented as Paper 70-1136 at the AIAA 8th Electric Propulsion Conference, Stanford, Calif., August 31–September 2, 1970; submitted September 18, 1970; revision received November 9, 1970. The work reported in this paper was performed under NASA Contract NAS1-8090.

* Program Manager, Electrothermal Propulsion. Member AIAA.

† Senior Project Engineer, Electrothermal Propulsion. Member AIAA.

‡ Project Engineer, Electrothermal Propulsion.

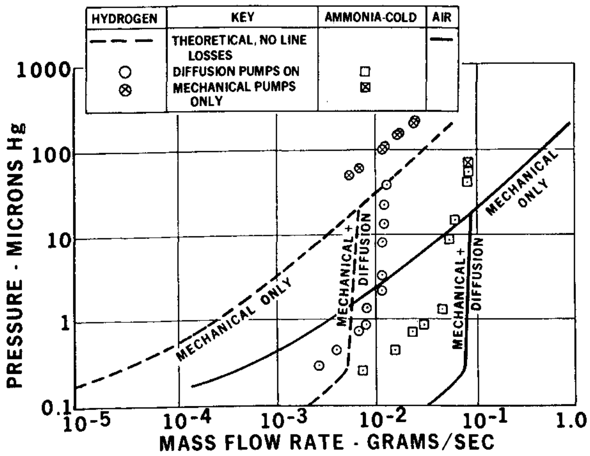

Fig. 1 High-vacuum test facility pumping capacity.

nated with over 8000 hr on the ammonia thrusters. Table 1 summarizes the nominal performance values obtained with the life test thrusters.

Details of the completed life test, including post-test metallographic examinations of three of the thrusters and performance calibrations of all of the thrusters, are described in Ref. 2. With the exception of thrusters S-1 and S-2, pre-test and post-test calibrations were in acceptable agreement. Sublimation of the heater parts and nozzle, and changes in nozzle throat geometry due to erosion or deposition, were insignificant. These factors, therefore, were not considered life determining criteria in the life tested design.

High-Vacuum Tests

During the resistojet life test cell pressure P was 10 μ or greater, and it was observed that as P was decreased below 100 μ, a substantial improvement in thrust was achieved. As a consequence, upon the completion of the life test, a new high-vacuum facility was installed at Marquardt, capable of testing 10-mlb resistojets to $\sim 0.5\ \mu$. The pumping capacity of this facility is shown in Fig. 1. Vendor theoretical curves for air are shown by the solid line. Hydrogen theoretical performance is shown as a dotted line and has been scaled from the air curves by the ratio of molecular weights of the two gases. Actual data points for H_2 and nondissociated NH_3 are plotted.

The reason for the improved thrusting performance at $P < 100\ \mu$ is not fully understood. The life-test thrusters had convergent-divergent nozzles with exit-to-throat area ratios of about 30. Nozzle flow in the 10-mlb resistojet is completely viscous with throat-diameter Reynolds numbers of about 400 and 800, respectively, for H_2 and NH_3. A significant subsonic layer exists along the nozzle walls. It would seem that cell pressures could propagate upstream into the divergent nozzle via this subsonic layer. Increasing cell pressure could thicken this layer, effectively reduce the expansion ratio, and thereby, effect a reduction in specific impulse.

Table 2 Magnitude of cell pressure effects

Propellant	Effect	Force, g	Change in specific impulse, %
H_2, NH_3	PA force at 1000μ	0.07	−1.6
H_2	Windage, maximum at 10μ	0.09	−2
H_2	Viscous-nozzle 0.5 to 1000μ	0.89	−19
NH_3	Windage, maximum at 5μ	0.09	−2
NH_3	Viscous-nozzle 0.5 to 1000μ	0.75	−17

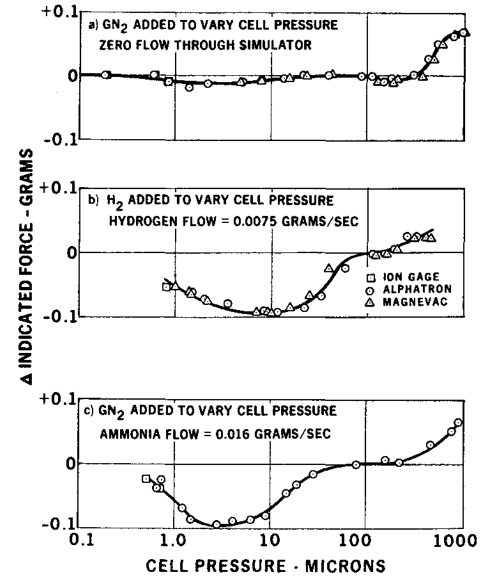

Fig. 2 Test chamber windage effect.

Gas flow within the cell (windage) has been considered to be another source of observed thrust variation; i.e., circulation induced by the thruster exhaust plume imposes a force by momentum exchange with the thrust stand and thrusters. Thruster B-2 was tested in the high-vacuum facility to evaluate these suspected cell pressure effects.

To determine whether a windage effect existed, a resistojet flow simulator was operated adjacent to the B-2 thruster. The thruster was mounted on the thrust stand. The simu-

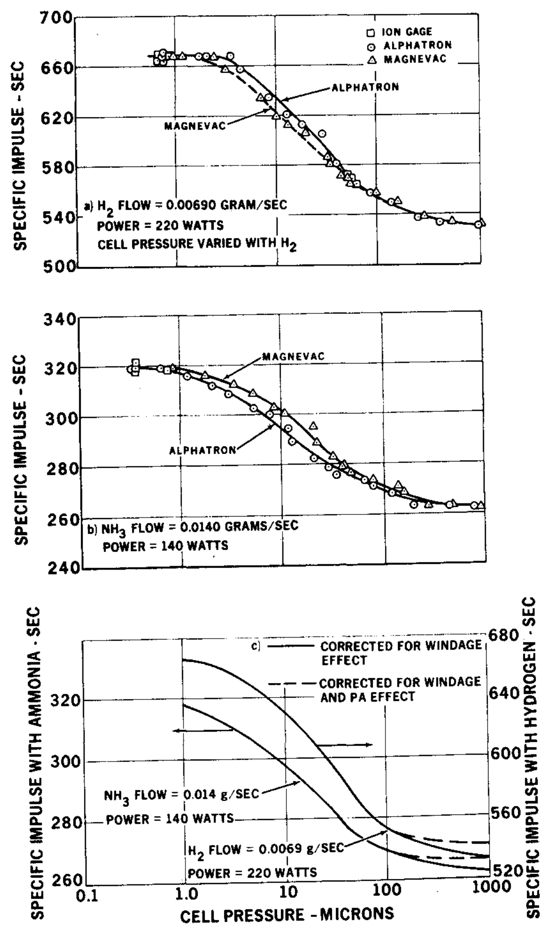

Fig. 3 Resistojet thruster cell pressure effect.

lator, consisting of a resistojet size nozzle which would simulate a thruster plume, was not attached to the thrust stand. Cell pressure P was varied by adding nitrogen gas (GN_2) away from the thrust stand to minimize its spouting velocity effect on winds in the cell. Propellant flow was introduced through the simulator while propellant to the thruster was turned off. Figure 2a presents a reference calibration to show the effect of P without simulator flow on the thrust readings. These data indicate that the thrust stand is relatively unaffected (less than 0.01 g) by the test chamber gases until $P \simeq 300\ \mu$ is reached. Thereafter, an increasingly strong positive force is indicated as P in increased. This is a facility-pumping-system-induced phenomenon, and it occurred in all data taken. (The "no simulator flow" calibration was repeated using hydrogen to vary cell pressure with similar results.)

Figures 2b and 2c show the results of typical resistojet flows using H_2 and NH_3 with the simulator. A significant negative force is observed for $P < 100\ \mu$. The windage force curves are similar for both propellants reaching maximum negative values of about 0.1 g. The maximum negative force for NH_3 occurs at a lower P than for H_2. The windage forces can be converted to effective specific impulse (I_{sp}) reduction by dividing by the mass flow rate. Thus, for the 0.1-g maximum negative force, corresponding I_{sp} reductions are 13 and 6.2 sec, respectively, for H_2 and NH_3 propellants. The windage force is repeatable for a given set of thruster/thrust-stand/test-chamber characteristics and for a given method of introducing bleed gas and given pumping station characteristics. It must be redetermined if any of these factors are changed.

Figures 3a and 3b present data for a range of cell pressure of three orders of magnitude for H_2 and NH_3 propellants, respectively. These data have been corrected for windage effects. Mass flow rate is constant in each case, and maximum specific I_{sp} corresponds closely to the design thrust of 10 mlb. These data indicate typical life-test conditions with respect to power and mass flow rate conditions but are not to be interpreted as thruster maximum capability.

In Fig. 3c the solid lines correspond to mean fits to the data in Figs. 3a and 3b. Note that different ordinate scales are used for hydrogen and ammonia propellant cases. Dotted lines are introduced to show a cell pressure times nozzle exit area (PA) force correction. The final curves corrected for windage and PA forces represent what can be termed a viscous-nozzle effect.

The magnitude of the three cell pressure effects (windage, PA force, and viscous-nozzle) of Fig. 3c are tabulated in Table 2. The percentage effects of these forces on hard-vacuum ($0.5\ \mu$) specific impulse are also tabulated. As evidenced by these data, the windage and PA force are second-order compared to the viscous-nozzle effect.

Post-Life-Test Performance

Several high-temperature performance runs were made on the B-2 thruster in the high-vacuum facility and are described in Table 3. These data were obtained after the B-2 thruster had been life-tested in excess of 6000 hr (more than 6000 duty cycles). For comparison, the life-test data of Ref. 2 indicated over-all total power efficiencies as follows: 1) 51% at 640-sec specific impulse on hydrogen propellant, and 2) 42% at 320-sec specific impulse on ammonia propellant. These values correspond to life-test cell pressures for which a cell-pressure penalty occurred. A significant improvement in efficiency as a result of the lower P is reflected in the Table 3 values.

Table 3 B-2 thruster high-vacuum cell performance

Propellant	Thrust, g	Specific impulse, sec	Electric power, w	Over-all-total power efficiency[a]
H_2	4.48	634	180	0.65
H_2	4.60	669	221	0.59
H_2	4.85	686	227	0.62
H_2	5.85	625	235	0.64
NH_3	4.42	320	141	0.45
NH_3	5.23	326	169	0.46

[a] Over-all total power efficiency: $\eta \triangleq$ (thrust) $\times$ (specific impulse)/20.8 $\times$ (total power) where total power is the sum of the initial power in the propellant gas and the applied electric power.

Specific impulse of the resistojet is an indication of the chamber gas temperature entering the thruster nozzle. The Table 3 data suggest chamber temperatures ranging from 1700° to 2100°K for hydrogen and about 1900°K for ammonia. Metallographic examinations of the heating elements of the life tested thrusters show[2] that an adverse temperature distribution existed in the concentric tubes heater. Gas flow suffered an actual cooling effect in the last heater passage. Structural temperatures had to be higher for a given I_{sp} than they would had the temperature gradient been favorable. The adverse temperature distribution results in a lower efficiency and higher power consumption than for the same I_{sp} in a thruster with a favorable distribution.

An improved resistojet, currently under development, has a contoured heater element which will give a more favorable temperature distribution, thereby permitting higher I_{sp} and efficiency for a given limit on maximum structural temperature. For a maximum structural temperature of 2400°K, we predict 66% efficiency at 700-sec specific impulse for hydrogen and 50% efficiency at 340 sec for NH_3.

References

[1] Halbach, C. R. and Yoshida, R. Y., "Development of a Biowaste Resistojet," AIAA Paper 70-1133, Stanford, Calif., 1970.

[2] Yoshida, R. Y. et al. "Resistojet Thruster Life Tests and High Vacuum Performance," Rept. CR-66970, 1970, NASA.

Spacer Effects on Lateral Heat Transfer in Multilayer Insulation

P. S. Jagannathan* and C. L. Tien†
University of California, Berkeley, Calif.

Lateral heat transfer plays an important role in the thermal performance of multilayer insulation systems.[1,2] For the case of an ideal dielectric (i.e., nonabsorbing and nonscattering) theoretical results agree well with the reported experimental data.[3] The spacers used in practice such as Dexiglas, Tissuglas, and others are, however, highly scattering and absorbing. Approximating them to ideal dielectrics may involve appreciable errors. This Note seeks an approximate analytical solution for the spacer effects. Special emphasis is placed on arriving at a solution which would make full use of the existing solutions for the case of nonabsorbing and nonscattering spacers.

Analysis

The system consists of two parallel conducting and radiating plates of finite length L and infinite width. The ends

Presented as Paper 70-849 at the AIAA 5th Thermophysics Conference, Los Angeles, Calif., June 29–July 1, 1970; submitted August 26, 1970; revision received October 16, 1970. Work supported by NASA Lewis Research Center under grant NGR-05-003-285.

* Department of Mechanical Engineering.

† Professor and Chairman, Department of Mechanical Engineering. Associate Fellow AIAA.